Biocatalysis and Biotransformation

ISSN: (Print) (Online) Journal homepage: https://www.tandfonline.com/loi/ibab20

Production of hydroxytyrosol from hydroxylation of tyrosol by *Rhodococcus pyridinivorans* 3HYL DSM109178

Jaouad Anissi, Khalid Sendide, Abdelkrim Ouardaoui, Mohammed Benlemlih & Mohammed El Hassouni

To cite this article: Jaouad Anissi, Khalid Sendide, Abdelkrim Ouardaoui, Mohammed Benlemlih & Mohammed El Hassouni (2021): Production of hydroxytyrosol from hydroxylation of tyrosol by *Rhodococcus pyridinivorans* 3HYL DSM109178, Biocatalysis and Biotransformation, DOI: 10.1080/10242422.2021.1903884

To link to this article: https://doi.org/10.1080/10242422.2021.1903884

BIOCATALYSIS AND BIOTRANSFORMATION
https://doi.org/10.1080/10242422.2021.1903884

Taylor & Francis
Taylor & Francis Group

RESEARCH ARTICLE

Production of hydroxytyrosol from hydroxylation of tyrosol by *Rhodococcus pyridinivorans* 3HYL DSM109178

Jaouad Anissi[a], Khalid Sendide[b], Abdelkrim Ouardaoui[b], Mohammed Benlemlih[c] and Mohammed El Hassouni[c]

[a]School of Engineering BIOMEDTECH, EUROMED University of Fes, Fez, Morocco; [b]Faculty of Sciences Dhar El Mahraz, Biotechnology, Environment, Agri-Food and Health Laboratory, Sidi Mohamed Ben Abdellah University, Fez, Morocco; [c]Laboratory of Biotechnology, School of Science and Engineering, Al Akhawayn University, Ifrane, Morocco

ABSTRACT

Hydroxytyrosol (4-(2-hydroxyethyl)-1,2-benzenediol) is the most known bioactive compound from the plant *Olea europaea* (olive tree). To date, few biocatalysis processes allowing efficient production of hydroxytyrosol from potential substrates including, tyrosol (2-(4-hydroxy) phenyl ethanol) and tyrosine have been reported. In this paper, we report for a Gram-positive bacterium that produces hydroxytyrosol via conversion of tyrosol and/or L-tyrosine, identified as a *Rhodococcus pyridinivorans* based on phenotypic characteristics and 16S rDNA sequence, and designated *R. pyridinivorans* strain 3HYL DSM109178. Interestingly, strain 3HYL shows an outstanding production of hydroxytyrosol from tyrosol up to 16.4 ± 0.23 mmol/L with high kinetic parameters exceeding the reported values. However, a slight downstream metabolism of the product is assigned to the wild-type strain during the stationary phase of growth. The plasmid-cured strain was obtained using random chemical mutagenesis, designated *R. pyridinivorans* 3HYL-AO, and was able to produce hydroxytyrosol, with yields up to 21.75 ± 0.34 mmol/L. Moreover, the plasmid-cured strain exhibited a significant reduction in the transformation to its acetic acid forms compared to the wild-type strain as depicted by HPLC analysis. Comparison of kinetic data of the bioconversion/accumulation process between the wild type and mutant strain, in the presence and absence of L-tyrosine, and thus suggesting the occurrence of an upstream pathway for synthesis of tyrosol via (L)-tyrosine.

ARTICLE HISTORY
Received 2 July 2019
Revised 5 February 2021
Accepted 11 March 2021

KEYWORDS
Rhodococcus pyridinivorans; de novo synthesis; biotransformation; hydroxytyrosol; tyrosol

Introduction

Hydroxytyrosol is an *o*-diphenol found in the olive tree and its products (Gordon et al. 2001), and it possesses several pharmacological activities (Ting et al. 2014; Colica et al. 2017). Data from *in vivo* and *in vitro* studies showed that hydroxytyrosol acts as antithrombotic by inhibition of LDL oxidation (Visioli et al. 1995), platelet aggregation (Petroni et al. 1995), and endothelial cell activation (Carluccio et al. 2003). Also, other reports have demonstrated the activity of hydroxytyrosol against multiple stages of the HIV-1 life cycle, inhibiting cell-to-cell HIV-1 transmission and viral core antigen p24 production (Lee-Huang et al. 2003). Other studies suggested that hydroxytyrosol might represent a non-toxic agent for the control of pro-inflammatory genes (Chiara Maiuri et al. 2005). Investigation on the protective effect of hydroxytyrosol on human melanoma cells exposed to UV-B radiation showed remarkable protection against such an effect (D'Angelo et al. 2005). Administration of a low dose of hydroxytyrosol, administered through olive mill wastewater, reduces the oxidative stress of rats exposed to passive smoking (Visioli et al. 2000), and improves blood lipid profile, antioxidant status, and reduces atherosclerosis development (González-Santiago et al. 2006). All investigations performed on various human cells have demonstrated that hydroxytyrosol exerts its antioxidant effect by scavenging hydrogen peroxide produced by human neutrophils (O'Dowd et al. 2004) and prevented oxidation in the erythrocytes (Manna et al. 1999).

Because of these properties, hydroxytyrosol has received much attention as an attractive chemical for both the pharmaceutical and food industries. Since the first findings of these pharmacological effects of hydroxytyrosol, interested scientists started to purify

CONTACT Jaouad Anissi j.anissi@ueuromed.org School of Engineering BIOMEDTECH, EUROMED University of Fes, Rond-point Bensouda, Route de Meknès, Fez BP 51, Morocco

Supplemental data for this article can be accessed here.

this molecule from its natural sources. For these reasons, several protocols and processes were developed. First attempts were directed towards the extraction and the purification of the hydroxytyrosol starting from the natural sources particularly from the olive tree and by-products.

The recovery and the purification of the hydroxytyrosol from olives and by-products require the use of a great amount of energy and toxic organic solvent and are time-consuming. Yet, because of the risk accompanied the use of pharmaceutical products produced chemically or by a treatment using toxic compounds such as solvents during the process, the development of a process for the production of hydroxytyrosol by using microbial cells, as biocatalyst is suitable for such products intended to pharmaceutical use.

Hydroxytyrosol (HT) has also been identified as a product of the oxidation of tyrosol by some bacteria, such as *Pseudomonas putida* F6 (Brooks et al. 2006), *Pseudomonas aeruginosa* (Allouche et al. 2004; Bouallagui and Sayadi 2018), *Serratia marcescens* (Allouche and Sayadi 2005) and *Halomonas* sp. strain HTB24 (Liebgott et al. 2007), or by using tyrosinase as a biocatalyst (Espín et al. 2001). Bacteria from the genus *Rhodococ*cus are known as versatile biocatalyst with an expanded spectrum of applications including biosynthesis and bioremediation. In his review, Finnerty (1992), has suggested bacteria belonging to the genus *Rhodococcus* as capable of oxidising a range of phenyl ethanol substrates, where tyrosol (4-(2-Hydroxyethyl)phenol), and since then, no experimental data dealing with the occurrence of such process among species of the genus *Rhodococcus* are available. In the present work, we describe a species, designated as strain 3HYL and belonging to the genus *Rhodococcus* based on biochemical and molecular approaches. This strain displays, as well as its plasmid-free mutant, an *o*-hydroxylation efficiency of tyrosol and production of hydroxytyrosol with outstanding kinetic parameters. The process described in the present work is reproducible at a Lab bench scale and can be adapted to a pilot scale.

Materials and methods

Strain isolation and characterization

Soil samples were collected around an olive-tree (GPS coordinate: 33°54′6.79″ N, 4°39′45.47″ W) in a sterile plastic bottle. Subsequently, 1 g of soil was added to 100 mL of Luria Bertani broth (LB) and suspended under low ultrasound energy and agitation. 100 µL from the suspension were used to inoculate 100 mL of glucose-free M9 medium containing Na_2HPO_4 $7H_2O$, 34 g/L; KH_2PO_4, 15 g/L; NH_4Cl, 5 g/L; NaCl, 2.5 g/L; 2 mM $MgSO_4$; 0.1 mM $CaCl_2$, supplemented with 7.5 mmol/L tyrosol, 1 g yeast extract L^{-1}, and 0.1% (v/v) trace element solution containing: EDTA, 0.5 g/L; $ZnSO_4{\cdot}7H_2O$, 0.22 g/L; $CaCl_2$, 0.055 g/L; $MnCl_2{\cdot}5H_2O$, 0.05 g/L; $(NH_4)_6Mo_7O_{24}{\cdot}4H_2O$, 0.011 g/L; $CuSO_4{\cdot}5H_2O$, 0.016 g/L; $CoCl_2{\cdot}6H_2O$, 0.016 g/L, (w/v), pH 7.2. After 0, 12, 24, and 48 h of incubation at 37 °C, 100 µL from the culture dilutions were spread out on minimal medium agar supplemented with tyrosol at 15 mmol/L and incubated for 48 h at 37 °C. Strain characterization and identification data are shown in the Supplementary material. Standard tests were performed based on the descriptions of the genus by Jones and Goodfellow (2015). Cell morphology was examined using scanning electron microscopy as described by Kormendy (1975). Briefly, cells from the early exponential growth phase (1 day), stationary phase (2 days) in an LB culture, alongside those grown in the presence of tyrosol, were harvested and prepared as described by The growth of the isolate was monitored in a basal medium containing various concentrations of NaCl (0, 0.5, 1, 1.25, 1.5 and 2 M). The effect of increased tyrosol concentrations (0, 2.5, 7.5, 15, 22.5, 30, and 50 mmol/L) on the growth of strain 3HYL was tested in the same basal medium supplemented with yeast extract (1 g/L). Temperatures between 15 and 55 °C at 5 °C intervals and pH values ranging from 2 to 12 in one-unit intervals were tested on a basal medium containing fructose at 200 mmol/L. Phenotypic properties of strain 3HYL were performed as described by Gordon et al. (1974). Further biochemical analyses were performed using API 20NE, API 50CH systems (BioMérieux, France) according to the manufacturer's instructions. Cell wall diamino-acids, sugars, and amino acid determinations were performed from the cell wall prepared by alkali treatment of washed cell pellets as described by Keddie and Cure (1977). Sugars determination was performed after hydrolysis in 1 mol/L HCl for 4 h. Amino acids and sugars were detected by thin-layer chromatography (TLC). For amino acids, TLC plates (cellulose with fluorescent indicator, obtained from Fluka, USA) were eluted using the mobile phase (methanol-water-6 N HCl-pyridine, 80-26-4-10), and the spots were visualised by spraying 0.2% ninhydrine (Staneck and Roberts 1974). Authentic DL- and DD-diaminopimelic acids (Sigma Chemical Co.), lysine, and ornithine were used as references for the analysis of diamino acids. For sugars, TLC plates (silica gel plates with fluorescent indicator, obtained from Fluka, USA) were eluted using the

mobile phase (butanol-acetic acid-water, 4-1-1), and the spots were visualized after spraying with thymol/H_2SO_4 and incubation at 110 °C. Standards of galactose, arabinose, glucose, xylose, rhamnose, maltose, and ribose were used as references for the sugar analysis.

16s rDNA sequencing and phylogenetic analysis

The genomic DNA of strain 3HYL was extracted and purified using PureLink™ Genomic DNA Kit (Invitrogen) following the manufacturer's instructions. The universal primers, 1492 R (GGCTACCTTGTTACG ACTT) and 8 F (AGAGTTTGATCCTGGCTCAG) were used to amplify a 16S rDNA fragment of more than 1400 bp. PCR was performed in a thermal cycler (Techne Genius, Model FGEN05TD, England). The PCR conditions were set as described by Turner et al. (1999). Sanger sequencing was performed at the Centre of Innovation (USMBA-Fez, Morocco) using an ABI PRISM 3130XL Genetic Analyser (Applied Biosystems). The 16S rDNA assembled sequence was analyzed by search in the NCBI database. The phylogenetic relationship with other similar strains was done by applied Neighbor-Joining (NJ) criteria, using the MEGA X software (Kumar et al. 2018). Phylogeny tests were assessed by bootstrapping with 1000 replicates, the maximum likelihood composite was used as a substitution model.

Fermenter set-up and growth conditions

Batch fermentation was carried out in a 5 L bioreactor (Biostat B, Sartorius-Germany) with a total working volume of 4 L containing a two-phase ferment. The growth temperature was 37 °C, the pH was maintained at 7.2 by adjusting with 0.5 M HCl and 0.5 M NaOH aqueous solutions, the agitation speed was set between 5 rpm/min and 350 rpm/min, and the gassing rate was adjusted between 0 L/h and 7 L/min air. The dissolved oxygen concentration was monitored using a standard amperometric pO_2 probe (Mettler-Toledo Prozeûanalytik GmbH, Stein-Bach, Germany) with a 12 mm O_2 sensor. Strain 3HYL was grown in M9 medium, supplemented with 15 mmol/L tyrosol and 0.6% casamino acids solution and with 1% (v/v) of a solution of trace elements of the composition described above. Finally, the pH of the medium was adjusted to 7.2 with 0.5 M HCl and 0.5 M NaOH aqueous solutions. All solutions were filter-sterilized (0.2 μm, MILLIPORE). Cultures were inoculated with 1 mL of 2×10^3 cells/mL pre-grown in an LB medium in a rotatory shaker at 180 rpm at 37 °C. The growth rate was monitored by measuring the turbidity at 600 nm. Samples (1 mL), from the culture medium, were collected at 1 h intervals and clarified through a 0.2 μm filter (MILLIPORE), for quantitative analysis.

Kinetic determination of hydroxytyrosol production

HPLC was performed using an LCQ Advantage Max Thermo Electron. The separation was carried out in a BDS Hypersil C18 column (150 × 4.6 mm × 5 μm). The mobile phase consisted of acetonitrile–H_3PO_4 (10:0.1%) where the concentration of acetonitrile varied as follows: at 0 min, 10%; from 0 min to 20 min, from 10 to 50%; and hold for 5 min; from 25 to 30 min from 50 to 10%. The column temperature was maintained at 40 °C, and the flow rate was 0.5 mL/min. A standard curve for quantitative measurements was made from 0 ppm to 10^3 ppm using HT as a standard. Compounds were identified by comparing their retention times with those of authentic samples (tyrosol, R_t = 13.12–13.15; hydroxytyrosol, R_t = 10.07–10.26; DHPA, R_t = 16.52–16.55). The GC-MS analysis was used for the mass identification of HT. A Thermo Scientific ISQ™ LT Single Quadrupole GC-MS System was used. The carrier gas was helium (99.99% purity), used at a flow rate of 1.5 mL/min. The oven temperature program was as follows: from 65 °C to 100 °C at a ramp of 10 °C/min, from 100 to 260 °C at 4 °C/min, and 10 min at 260 °C. A sample from the culture medium (1 mL) was extracted with ethyl acetate, and 100 μL of bis (trimethylsilyl) trifluoroacetamide (BSTFA) was added to 100 μL of the organic extract. The obtained solution was incubated for 20 min at 80 °C. Ethyl acetate and BSTFA were evaporated under an N_2 current and the residue was dissolved n ethyl acetate (1 mL) and analyzed by GC-MS. TLC analysis was carried out using silica gel sheets (DC-Alufolien-Kieselgel, 2 mm layer, (Fluka) using a mixture solvent containing ethyl acetate, chloroform, and acetic acid (50:49:1). The spots were visualised either by exposure to UV light or by spraying a solution of methanol containing 1% $FeCl_3$. Total phenolic compounds were quantified using a modification of the method described by Singleton and Rossi (1965). Briefly, 100 μL of cell-free supernatant were mixed with 0.25 mL of Folin–Ciocalteu reagent, then 500 μL of 20% (w/v) sodium carbonate solution and 4 mL water were added, and the mixture was vortexed thoroughly. After 30 min, colour development was measured at 725 nm using a JASCO V-350 spectrophotometer

(USA). Authentic HT was used as a standard for the calibration curve. Total phenolic compounds were expressed as mg gallic acid equivalent per mL of the cell-free medium. All measurements were performed in triplicate. Kinetic parameters were calculated as follows:

Q_{pmax} (mmol/L/h) designs the production rate, calculated as the maximum concentration of hydroxytyrosol divided by the total culture time. μ_{pmax} (h^{-1}) defines the maximum rate of production, and calculated as the logarithm variation of the product concentration as a function of the time and divided by the corresponding biomass considered as the corresponding optical density. μ_{xmax} (h^{-1}) defines the maximum growth rate and is calculated as the logarithm variation of the biomass (optical density) divided by the time course. $R_{p/s}$, which defines the stoichiometry of the process of hydroxylation of tyrosol. It is calculated as the difference between the maximal and initial concentration of the hydroxytyrosol divided by the difference between the initial and the final concentration of the substrate.

Plasmid curing and production assay

In all the experiments, exponentially growing (log-phase) cells were used to ensure the sensitivity of mutagenesis. From a saturated culture, 1 mL is diluted into 500 mL fresh LB, and cells were grown at 37 °C for 6 to 7 h. The cell density was around 5×10^6 UFC/mL, then a range of concentrations of acridine orange (0–500 μg/mL) was added, and cells were additionally grown at 37 °C for a further 3 to 5 h. Samples were withdrawn during the time course of the mutagenesis experiment at 1 h intervals. Samples were plated on M9 medium supplemented with tyrosol at 7.5 mmol/L. Strains were screened for their ability to hydroxylate tyrosol and accumulate hydroxytyrosol.

Results and discussion

Strain isolation and identification

Typically, the bacterium is rod-shaped, having a size of 0.6–2 μm × 1–10μm, non-spore-forming, Gram-positive, non-motile. The morphology of the strain observed under scanning electron microscopy during the time course of the growth shows various morphologies, characterizes by branched mycelia during the early phase of growth and are subsequently divided into short rods through small cocci, thus defining the pleiotropic growth of species of the Nocardia (Figure S1). Colonies in LB agar medium are circular with a diameter of 1–1.5 mm, smooth and a little convex, and do show a pink pigment after 48 h at 37 °C. The isolate showed to be catalase, and urease positive, and oxidase negative. Table 1 shows a comparative table of key phenotypic characteristics of strain 3HYL and related species.

In contrast to most of the *Rhodococcus* species, from the 50 carbohydrates tested, the isolate was able to use for growth only fructose and aesculin after 24 h, and sorbitol after 72 h at 37 °C. The isolate shows the decomposition of (L)-tyrosine, adenine, and Tween-80. The temperature tolerated for the growth ranged from 20 °C to 42 °C, with an optimum at 37 °C. The isolate can support growth at a pH ranging from 6.00 to 8.75, with an optimum at pH 7.2. Growth under different salt concentration (NaCl) was between 0 and 85 g/L, with an optimum at 20 g/L.

The cell wall contains meso-diaminopimelic acid, arabinose, galactose, and glucose. The 16S rDNA sequence of the isolate was determined and deposited in the GeneBank database under accession no. FJ887962.1. The 16S rDNA sequence of strain 3HYL DSM109178 was 1420 nucleotides long. It was compared with available sequences of related species (retrieved from NCBI in April 2019). This sequence contains all the "signature" nucleotide characteristics of the family Nocardiaceae according to Stackebrandt

Table 1. Kinetic parameters of the conversion of tyrosol to hydroxytyrosol by *Rhodococcus pyridinivorans* 3HYL in different conditions.

	Substrate		Product				
	$Tyrosol_i$ (mmol/L)	$Tyrosol_f$ (mmol/L)	$Hydroxytyrosol_f$ (mmol/L)	Q_{pmax} (mmol/L/h)	μ_{xmax} (h^{-1})	μ_{pmax} (h^{-1})	$R_{p/s}$
Rhodococcus pyridinovorans 3HYL							
M9* + 6 g CAA L^{-1} microaerobic conditions	15.00	11.64 ± 1.32	14.65 ± 0.62	0.40 ± 0.05	0.28 ± 0.01	1.45 ± 0.52	3.36 ± 1.92
M9* + 6 g CAA L^{-1}in aerobic conditions	15.00	6.14 ± 0.43	13.45 ± 1.26	0.41 ± 0.02	0.82 ± 0.09	1.58 ± 0.67	2.85 ± 0.87
M9* + 1g/L yeast extract aerobic conditions	15.00	3.44 ± 0.75	9.31 ± 1.83	0.60 ± 0.03	0.98 ± 0.04	1.64 ± 0.23	1.03 ± 0.11
M9* + 0.2 g/L fructose in aerobic conditions	15.00	0.72 ± 0.26	10.75 ± 1.65	0.52 ± 0.03	0.31 ± 0.03	1.24 ± 0.65	1.06 ± 0.13

M9*: M9 minimal media supplemented with tyrosol at 15 mmol/L, Mg^{++} and Ca^{++} solution, trace elements as mentioned in material and methods; $tyrosol_i$: initial concentration of tyrosol; $tyrosol_f$: final concentration of tyrosol; $tyrosine_i$: initial concentration of tyrosine; $tyrosine_f$: final concentration of tyrosine; CAA: casamino acids®.

et al. (1997). In the tree-based Neighbor-Joining algorithm, strain 3HYL falls within the cluster comprising *Rhodococcus* species, and, in particular, forms a coherent cluster with the type strains of *R. pyridinivorans* strain NK19 and *R. rhodochrous* strain PRK1. The placement of the strain 3HYL within this cluster was also confirmed with the maximum-likelihood and maximum-parsimony algorithms. The 16S rDNA sequence similarity between strain 3HYL and the type strains of other validly described *Rhodococcus* species ranged between 99 and 94%. This strain has been designated *Rhodococcus pyridinivorans* strain 3HYL, and it was deposited at the DSMZ collection under the accession number DSM109178.

Data for strain identification are presented in Table S1, Figures S1 and S2.

Hydroxytyrosol production: kinetics of growth and production

Rhodococcus pyridinivorans strain 3HYL supports concentrations of tyrosol and hydroxytyrosol for optimum growth of 39.63 ± 2.37 mmol/L, and 46.27 ± 3.21 mmol/L, respectively. In mineral media containing tyrosol at 15 mmol/L, strain 3HYL DSM109178 shows an outstanding production of HT with maximum concentrations up to 13.45 ± 1.26 mmol/L after 8 h of incubation under aerobic conditions.

Figure 1 showed the evolution of the concentrations of both, tyrosol and hydroxytyrosol during the growth of strain 3HYL. It shows that the sum of the produced hydroxytyrosol and the present tyrosol at a time *t*, during the exponential phase of the growth is by far superior to 15 mmol/L, reaching values up to 25.72 ± 1.43 mmol/L. These data were validated based on HPLC-UV analysis using tyrosol as the standard ($R^2 = 0.985$). Subsequently, kinetic experiments were conducted to determine parameters governing this unexpected conversion yield from tyrosol to hydroxytyrosol leading to an excess of both, the substrate and the product. The stoichiometry of the production of hydroxytyrosol via oxidation of tyrosol as indicated by the parameter $R_{p/s}$ in aerobic and micro aerobic conditions showed mean values of 3.36 ± 1.92 and 2.85 ± 0.87, respectively (See Table 1 and Figure 2(A)), indicating that the production reaction is not equimolar. However, the oxygenation rate did not show any effect on the production rate Q_{pmax} (mmol/L/h) that shows positive dependency to the initial density of inoculum (Figure 2(B)). In contrast, cultivation in mineral medium containing only tyrosol (15 mmol/L), and fructose (25 mmol/L) as a supplement source of carbon, did show a stoichiometric depletion of tyrosol along with the production of hydroxytyrosol compared to culture in mineral medium containing tyrosol, and a supplement source of amino acids (e.g. Yeast extract, Casaminoacids) under the same conditions (Table 1). Furthermore, monitoring the total phenolic compounds from the cell-free supernatant during the growth of the isolate *Rhodococcus pyridinivorans* strain 3HYL in M9 minimal medium containing tyrosol showed a significant increase in the total phenolic concentration (See Figure S3), reaching values up to 24.31 ± 1.43 mmol/L tyrosol equivalent, when compared to *Pseudomonas aeruginosa* strain ET6 that in contrast, it exhibits instead a catabolic metabolism of tyrosol via hydroxytyrosol.

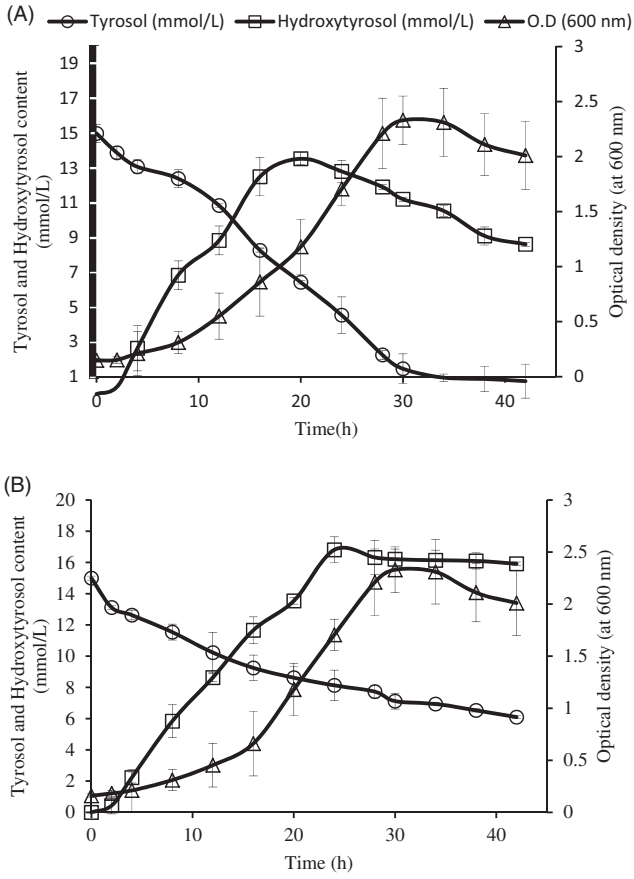

Figure 1. Time course of hydroxytyrosol, tyrosol and biomass concentrations. Values were calculated based on HPLC quantitation. (A): culture performed under oxygenation rate of 7 L/min and under agitation of 250 rev/min, (B): culture performed under oxygenation rate of 0.2 L/min and under agitation of 30 rev/min. (■): hydroxytyrosol, (●): tyrosol, (▲): optical density. Culture conditions are as described in material and methods.

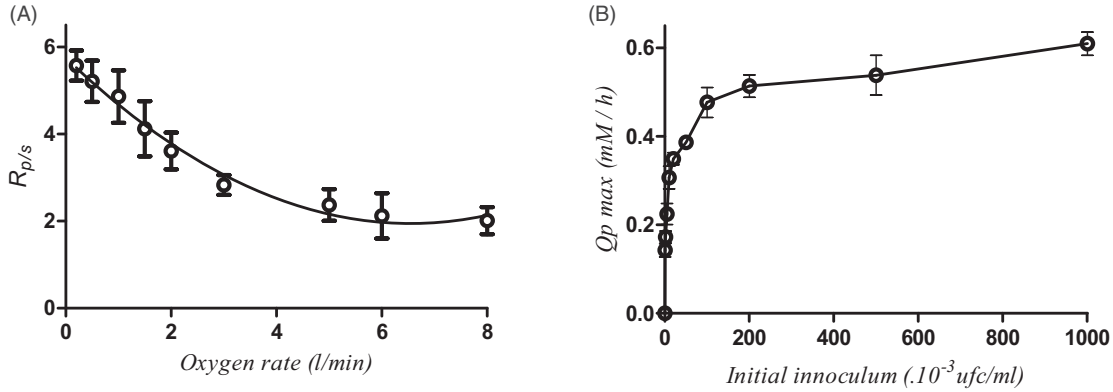

Figure 2. (A), Effect of the oxygen rate (L/min) on the kinetic parameter $R_{p/s}$, calculated as the difference between the final and initial concentration of the hydroxytyrosol, assumed as the maximal hydroxytyrosol concentration in the cell-free medium during the steady state and divided by the difference between the initial and the final concentration of the substrate in the same conditions as before. (B) Evolution of the Q_{pmax} (mM/h) as function of the initial inoculum density, calculated as the maximum concentration of hydroxytyrosol divided by the total culture time.

Table 2. Kinetic parameters of the conversion of tyrosol to hydroxytyrosol by *Rhodococcus pyridinivorans* 3HYL and strain 3HYL-AO1.

	Substrates				Product				
	Tyrosol$_i$ (mmol/L)	Tyrosine$_i$ (mmol/L)	Tyrosine$_f$ (mmol/L)	Tyrosol$_f$ (mmol/L)	Hydroxytyrosol$_f$ (mmol/L)	Q_{pmax} (mmol/L/h)	μ_{xmax} (h^{-1})	μ_{pmax} (h^{-1})	$R_{p/s}$
Rhodococcus pyridinovorans 3HYL									
M9* + 6 g/L CAA	7.50	7.50	ND	2.77 ± 0.34	12.40 ± 0.81	0.41 ± 0.74	0.30 ± 0.04	1.19 ± 0.05	2.01 ± 0.28
M9* + 6 g/L CAA I+ 0.05% tyrosine	7.50	7.50	0.24 ± 0.00	5.06 ± 0.27	20.01 ± 0.64	0.60 ± 0.73	0.89 ± 0.01	1.58 ± 0.03	5.57 ± 0.13
M9* + 1 g/L yeast extract	7.50	7.50	ND	8.27 ± 0.13	16.81 ± 0.21	0.69 ± 0.02	0.59 ± 0.04	3.15 ± 0.12	2.50 ± 0.11
Rhodococcus pyridinovorans 3HYL-AO1									
M9* + 6 g/L CAA	2.50	7.50	ND	10.99 ± 0.21	18.75 ± 0.56	0.62 ± 0.08	0.94 ± 0.03	1.64 ± 0.11	2.48 ± 0.12
M9* + 6 g/L CAA + 0.05% tyrosine	2.50	7.50	0.17 ± 0.00	9.54 ± 0.52	23.50 ± 0.27	0.65 ± 0.02	0.45 ± 0.04	1.83 ± 0.04	4.68 ± 0.134
M9* + 1 g/L yeast extract	2.50	7.50	ND	3.95 ± 0.14	21.75 ± 0.34	0.52 ± 0.01	0.34 ± 0.01	1.24 ± 0.02	1.97 ± 0.25

M9*: M9 minimal media supplemented with tyrosol at 15 mmol/L, Mg^{++} and Ca^{++} solution, trace elements as mentioned in material and methods; tyrosol$_i$: initial concentration of tyrosol; tyrosol$_f$: final concentration of tyrosol; tyrosine$_i$: initial concentration of tyrosine; tyrosine$_f$: final concentration of tyrosine; CAA: casamino acids®.

Curing pHyl in Rhodococcus pyridinivorans 3HYL increased the accumulation of hydroxytyrosol

The improvement in HT accumulation by strain 3HYL is highly relevant for industrial applications. The wild type *Rhodococcus pyridinivorans* 3HYL yields up to 15.37 mmol/L HT in a fermentation media under optimal conditions. However, when using a plasmid-cured strain, obtained after iterative chemical mutagenesis with acridine orange, the mutated strain, designated *Rhodococcus pyridinivorans* 3HYL-AO1, showed production of up to 20.52 mmol/L of HT in the same conditions as the wild type. The plasmid-less strain 3HYL-AO1 showed an outstanding overall process with promising kinetic parameters of conversion of tyrosol to HT that exceed those recorded for the wild type, mainly the parameter *Rp/s* that describes the stoichiometry of the bioconversion of tyrosol to hydroxytyrosol (See Table 2 for details). This strain supports optimum tyrosol concentrations of 35.54 ± 2.61 mmol/L and a concentration of 28.62 ± 2.84 mmol/L of HT for optimum growth. Figure 3 displays the HPLC chromatograms of the cell-free supernatant during bioconversion of tyrosol to HT by *Rhodococcus pyridinivorans* 3HYL and *Rhodococcus pyridinivorans* 3HYL-AO1 at different time intervals. In contrast to the wild-type strain, that oxidises tyrosol to hydroxytyrosol, with concomitant formation of 3,4-Dihydroxyphenyl acetic acid (DHPA), the mutagenized strain shows a remarkable reduction in the synthesis of DHPA. Furthermore, *Rhodococcus pyridinivorans* 3HYL-AO1 shows an accumulation of HT to final concentration after 18 h of 21.75 ± 0.34 mmol/L, compared to the wild-type strain yielding 16.81 ± 0.21 mmol/L, as well as an increase in the parameters of production kinetic, as shown in Table 2.

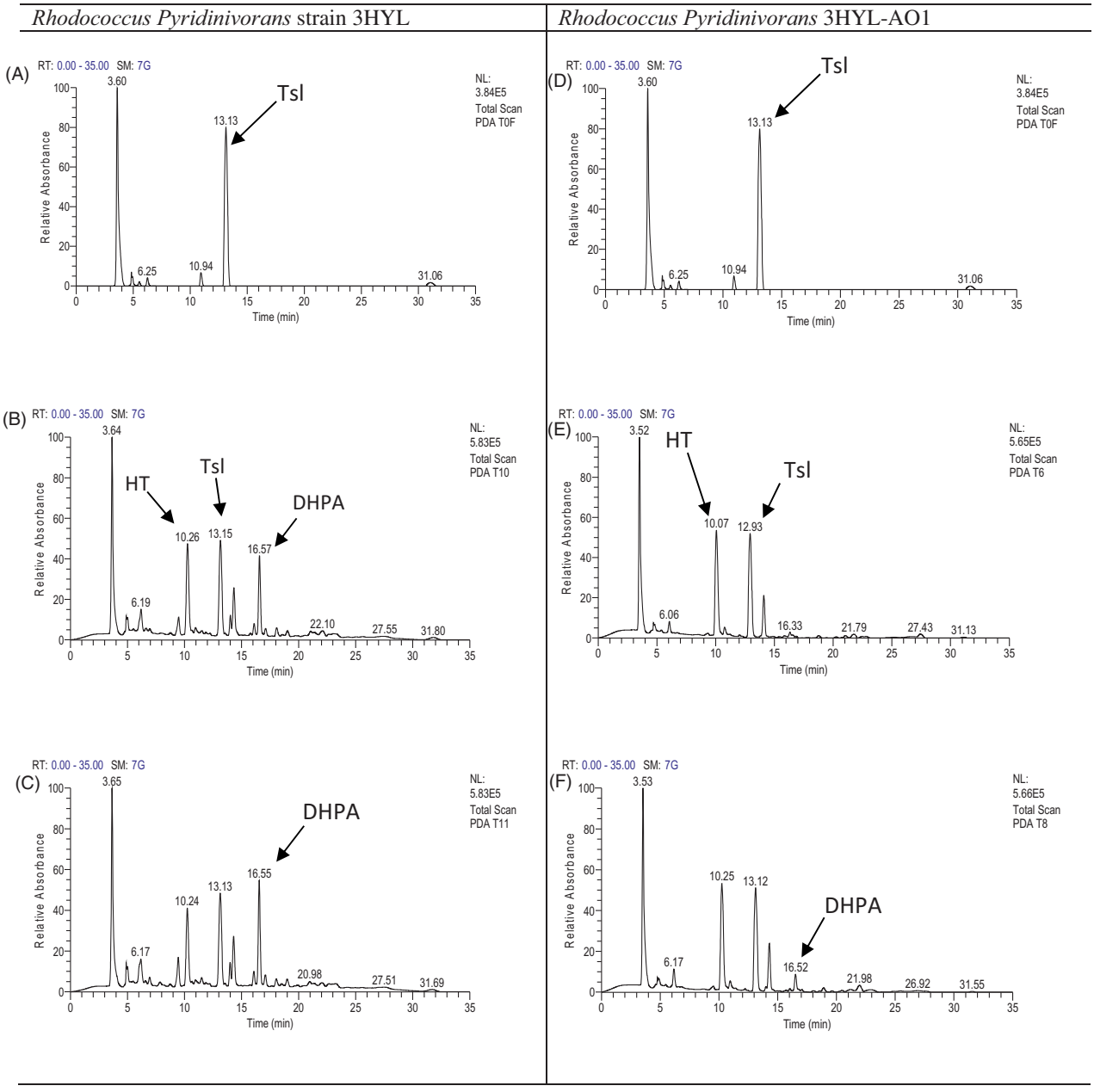

Figure 3. Typical HPLC chromatograms of cell-free medium showing the evolution of the composition of the culture medium during the growth *of Rhodococcus pyridinovorans* 3HYL (A–C), and *of Rhodococcus pyridinovorans* 3HYL-AO1 (D–F) in presence of tyrosol as substrate. (A and D): cell-free supernatant at time 0; (B, E): cell-free supernatant after 16 h of incubation; (C, F): cell-free supernatant after 48 h of incubation. Tsl: tyrosol, HT: hydroxytyrosol, and DHPA: 3,4-dihydroxyphenyl acetic acid.

Metabolism of tyrosol and hydroxytyrosol and the effect of tyrosine on the synthesis of tyrosol

Both, the wild-type and the mutated strain *Rhodococcus pyridinivorans* 3HYL-AO1 showed efficient hydroxylation of tyrosol to HT as well as the metabolism of tyrosine to hydroxytyrosol via tyrosol. Besides, HPLC analysis showed the appearance of other compounds, mainly resulting either from the pathway of the production of tyrosine to tyrosol or from the downstream metabolism of HT. GC-MS analysis of the TMS derivatives from the crude extract prepared from the cell-free medium showed signals of [M^+-3OTMS] and [M^+-2OTMS] at *m/z* 370.45, 384.04, and 282.34, corresponding to HT, 3,4-dihydroxyphenylacetic acid, and tyrosol, respectively, according to Di Tommaso et al. (1998). Standard compounds of HT, tyrosol, and 3,4-dihydroxyphenylacetic acid were used to verify the authenticity of the purified compounds. No

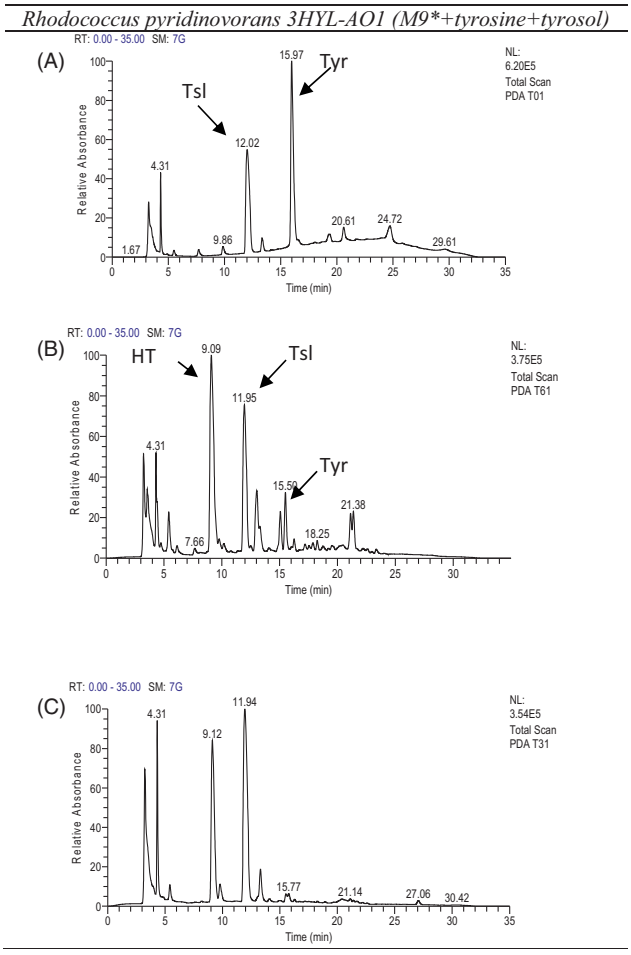

Figure 4. Typical HPLC chromatograms of cell-free medium showing the evolution of the production of hydroxytyrosol during the growth of *of Rhodococcus pyridinovorans* strain 3HYL-AO1 in presence of tyrosol and tyrosine as substratee. (A): cell-free supernatant at time 0 h; (B): cell-free supernatant after 12 h of incubation; and (C): cell-free supernatant after 24 h of incubation. Tsl: tyrosol, HT: hydroxytyrosol, and Tyr: tyrosine.

4-hydroxyphenylacetic acid (HPA) was detected in the cell-free medium. Both, HT and DHPA were subsequently metabolised to brown compounds, most likely due to tyrosinase activity allowing melanin synthesis from their corresponding quinones.

In the presence of (L)-tyrosine (7.5 mmol/L) and tyrosol (2.5 mmol/L) in the production medium, both the wild-type and mutagenized strain (5.5×10^6 UFC/mL) consume almost all tyrosine within 16 h of culture with the concomitant production of both tyrosol and HT. The concentration of the later increases to reach values up to 20.01 ± 0.68 mmol/L for *Rhodococcus pyridinivorans* 3HYL and 23.50 ± 0.24 mmol/L for *Rhodococcus pyridinivorans* 3HYL-A01. Table 2 summarises the kinetic parameters of the production of hydroxytyrosol in the presence and absence of tyrosine and Figure 4 displays the HPLC chromatograms by strain *Rhodococcus pyridinivorans* 3HYL-AO1 and the corresponding kinetic parameters. In the condition of the growth of wild type and the plasmid-cured mutant in the presence of tyrosine as well as tyrosol, the parameter *Rp/s* showed values of 5.57 ± 0.13 and 4.68 ± 0.134, yielding thus, 20.01 ± 0.64 mmol/L and 23.50 ± 0.27 mmol/L, respectively (see Table 2). When grown in the presence of (L)-tyrosine, both the wild-type and the mutated strain of *Rhodococcus pyridinivorans* 3HYL showed efficient production of both tyrosol and HT with kinetic parameters higher than those registered in the absence of (L)-tyrosine. Yet, these data corroborate with the involvement of a *de novo* pathway with (L)-tyrosine as a precursor for tyrosol synthesis, as well as the hydroxylation reaction to allow hydroxytyrosol production in the culture media (Figure 5). In comparison to what has already been suggested for other biocatalysts (Allouche et al. 2004; Allouche and Sayadi 2005; Brooks et al. 2006; Bouallagui and Sayadi 2018), Table S2, strain 3HYL shows during the higher production yield late exponential phase of growth of either the wild-type or the mutated strain of *Rhodococcus pyridinivorans* 3HYL in presence of tyrosol, the culture medium turns brown, indicating the formation of melanin from the corresponding *o*-quinones.

In contrast to the wild type, *Rhodococcus pyridinivorans* 3HYL-AO1 showed production and accumulation of HT with reduced DHPA formation, thus allowing easy purification of HT and tyrosol from the cell-free medium. Additionally, no HPA was detected in the culture media during the biotransformation process, compared to most of the described biocatalysts, indicating that the formation of the corresponding carboxylic acid occurs after the *o*-hydroxylation of tyrosol. This suggests that the HPA pathway is not active, in contrast to what has been demonstrated for *Rhodococcus globerulus* PWD1 (Stackebrandt et al. 1997).

Conclusion

In conclusion, this process of the production of hydroxytyrosol via hydroxylation of tyrosol using either the wild type or the plasmid-cured strain of *Rhodococcus pyridinivorans* 3HYL is unique in that it allows the production and accumulate HT at concentrations up to 23.01 ± 2.37 mmol/L in the cell-free medium and it does so with high kinetic parameters, which makes it suitable for industrial production of hydroxytyrosol, which is easy to isolate from production medium. The occurrence of a *de novo* pathway

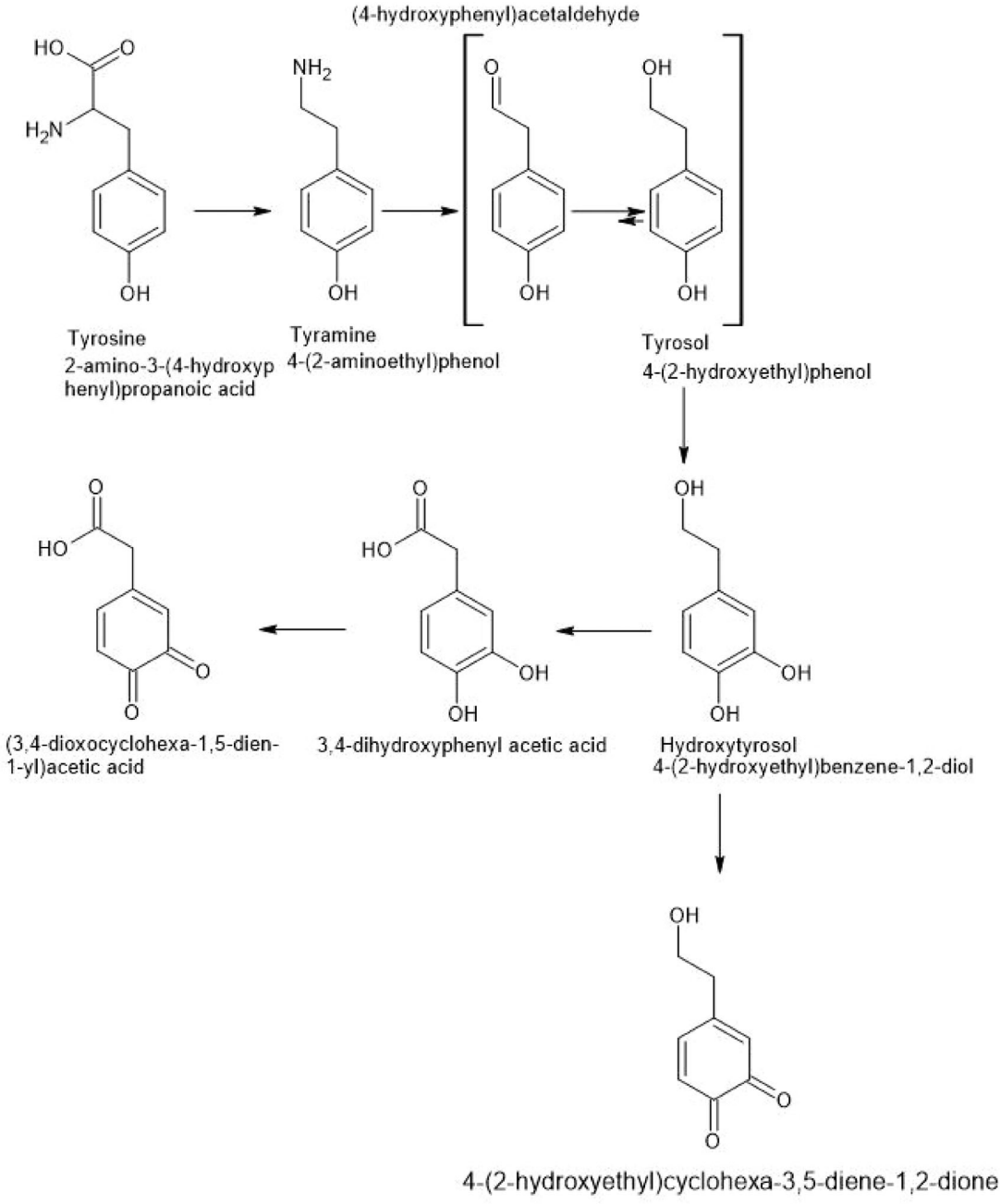

Figure 5. Proposed pathways displayed during bacterial production of hydroxytyrosol from tyrosol and tyrosine.

for the synthesis of tyrosol is supported by the increase in the $R_{p/s}$ parameter that exceeds one in most optimal cases. The optimized hydroxylation of the tyrosine process, in combination with a supply of tyrosine as a supplement substrate, enables the producing hydroxytyrosol at high levels of quantity and purity. Moreover, in the presence of tyrosine, these parameters showed relatively higher values for the mutant compared to the wild-type, showing significant improvement in product yield, thereby increasing the cost-effectiveness of the process. These results gave insights into the study of the governing pathway for the *de novo* synthesis of tyrosol and provide hints for modelling the kinetic parameters governing the bioconversion of tyrosol to hydroxytyrosol by the isolate *Rhodococcus pyridinivorans* strain, which are subjects to ongoing projects. This process opens the way for the economic and environmentally friendly production of hydroxytyrosol.

Acknowledgements

The authors are thankful to Dr. Jaouad Shikh Lahlou from COOPER Maroc S.A, for providing us with pure

hydroxytyrosol. Also, the authors are thankful to Dr. Violetta Cavallei from Al Akhawayn University for reviewing the English of the present paper.

Disclosure statement

No potential conflict of interest was reported by the author(s).

References

Allouche N, Damak M, Ellouz R, Sayadi S. 2004. Use of whole cells of *Pseudomonas aeruginosa* for synthesis of the antioxidant hydroxytyrosol via conversion of tyrosol. Appl Environ Microbiol. 70(4):2105–2109.

Allouche N, Sayadi S. 2005. Synthesis of hydroxytyrosol, 2-hydroxyphenylacetic acid, and 3-hydroxyphenylacetic acid by differential conversion of tyrosol isomers using *Serratia marcescens* strain. J Agric Food Chem. 53(16):6525–6530.

Bouallagui Z, Sayadi S. 2018. Bioconversion of *p*-tyrosol into hydroxytyrosol under bench-scale fermentation. Biomed Res Int. 2018:7390751.

Brooks SJ, Doyle EM, O'Connor K. 2006. Tyrosol to hydroxytyrosol biotransformation by immobilised cell extracts of *Pseudomonas putida* F6. Enzyme. Microb. Technol. 39(2): 191–196.

Carluccio MA, Siculella L, Ancora MA, Massaro M, Scoditti E, Storelli C, Visioli F, Distante A, De Caterina R. 2003. Olive oil and red wine antioxidant polyphenols inhibit endothelial activation: antiatherogenic properties of mediterranean diet phytochemicals. Arterioscler Thromb Vasc Biol. 23(4):622–629.

Chiara Maiuri M, De Stefano D, Di Meglio P, Irace C, Savarese M, Sacchi R, Cinelli MP, Carnuccio R. 2005. Hydroxytyrosol, a phenolic compound from virgin olive oil, prevents macrophage activation. Naunyn Schmiedebergs Arch Pharmacol. 371(6):457–465.

Colica C, Di Renzo L, Trombetta D, Smeriglio A, Bernardini S, Cioccoloni G, Costa de Miranda R, Gualtieri P, Sinibaldi Salimei P, De Lorenzo A, et al. 2017. Antioxidant effects of a hydroxytyrosol-based pharmaceutical formulation on body composition, metabolic state, and gene expression: a randomized double-blinded, placebo-controlled crossover trial. Oxid Med Cell Longev. 2017:2473495.

D'Angelo S, Ingrosso D, Migliardi V, Sorrentino A, Donnarumma G, Baroni A, Masella L, Tufano MA, Zappia M, Galletti P, et al. 2005. Hydroxytyrosol, a natural antioxidant from olive oil, prevents protein damage induced by long-wave ultraviolet radiation in melanoma cells. Free Radic Biol Med. 38(7):908–919.

Di Tommaso D, Calabrese R, Rotilio D. 1998. Identification and quantitation of hydroxytyrosol in Italian wines. J High Resol Chromatogr. 21(10):549–553.

Espín JC, Soler-Rivas C, Cantos E, Tomás-Barberán FA, Wichers HJ. 2001. Synthesis of the antioxidant hydroxytyrosol using tyrosinase as biocatalyst. J Agric Food Chem. 49(3):1187–1193.

Finnerty WR. 1992. The biology and genetics of the genus *Rhodococcus*. Annu Rev Microbiol. 46:193–218.

González-Santiago M, Martín-Bautista E, Carrero JJ, Fonollá J, Baró L, Bartolomé MV, Gil-Loyzaga P, López-Huertas E. 2006. One-month administration of hydroxytyrosol, a phenolic antioxidant present in olive oil, to hyperlipemic rabbits improves blood lipid profile, antioxidant status and reduces atherosclerosis development. Atherosclerosis. 188(1):35–42.

Gordon RE, Barnett DA, Handerhan JE, Pang CHN. 1974. Nocardia coeliaca, Nocardia autotrophica, and nocardin strain. Int. J. Syst. Bacteriol. 24(1):54–63.

Gordon MH, Paiva-Martins F, Almeida M. 2001. Antioxidant activity of hydroxytyrosol acetate compared with that of other olive oil polyphenols. J Agric Food Chem. 49(5): 2480–2485.

Jones AL, Goodfellow M. 2015. Rhodococcus. In: Bergey's manual of systematics of archaea and bacteria. Hoboken (NJ): Wiley; p. 1–50.

Keddie RM, Cure GL. 1977. The cell wall composition and distribution of free mycolic acids in named strains of coryneform bacteria and in isolates from various natural sources. J Appl Bacteriol. 42(2):229–252.

Kormendy AC. 1975. Microorganisms. In: Principles and techniques of scanning electron microscopy. New York (NY): Van Nostrand Reinhold; p. 82–108.

Kumar S, Stecher G, Li M, Knyaz C, Tamura K. 2018. MEGA X: Molecular Evolutionary Genetics Analysis across computing platforms. Mol Biol Evol. 35(6):1547–1549.

Lee-Huang S, Zhang L, Lin Huang P, Chang Y-T, Huang PL. 2003. Anti-HIV activity of olive leaf extract (OLE) and modulation of host cell gene expression by HIV-1 infection and OLE treatment. Biochem. Biophys. Res. Commun. 307(4):1029–1037.

Liebgott PP, Labat M, Casalot L, 2007. Bioconversion of tyrosol into hydroxytyrosol and 3,4-dihydroxyphenylacetic acid under hypersaline conditions by the new *Halomonas* sp. strain HTB24. FEMS Microbiol Lett. 276(1):26–33.

Manna C, Galletti P, Cucciolla V, Montedoro G, Zappia V. 1999. Olive oil hydroxytyrosol protects human erythrocytes against oxidative damages. The J. Nutri. Biochem. 10(3):159–165.

O'Dowd Y, Driss F, Dang PM, Elbim C, Gougerot-Pocidalo MA, Pasquier C, El-Benna J. 2004. Antioxidant effect of hydroxytyrosol, a polyphenol from olive oil: scavenging of hydrogen peroxide but not superoxide anion produced by human neutrophils. Biochem Pharmacol. 68(10): 2003–2008.

Petroni A, Blasevich M, Salami M, Papini N, Montedoro GF, Galli C. 1995. Inhibition of platelet aggregation and eicosanoid production by phenolic components of olive oil. Thromb Res. 78(2):151–160.

Singleton VL, Rossi JA. Jr 1965. Colorimetry of total phenolics with phosphomolybdic-phosphotungstic acid reagents. Am. J. Enol. Vitic. 3:144–158.

Stackebrandt E, Rainey FA, Ward-Rainey NL. 1997. Proposal for a new hierarchic classification system, *Actinobacteria classis* nov. Int. J. Syst. Evol. Microbiol. 47(2):479–491.

Staneck JL, Roberts GD. 1974. Simplified approach to identification of aerobic actinomycetes by thin-layer chromatography. Appl Microbiol. 28(2):226–231.

Ting H, Xiao-Wei H, Jian-Guo J, Xi-Lin X. 2014. Hydroxytyrosol and its potential therapeutic effects. J Agric Food Chem. 62(7):1449–1455.

Turner S, Pryer KM, Miao VPW, Palmer JD. 1999. Investigating deep phylogenetic relationships among cyanobacteria and plastids by small subunit rRNA sequence analysis. J Eukaryot Microbiol. 46(4):327–338.

Visioli F, Bellomo G, Montedoro G, Galli C. 1995. Low density lipoprotein oxidation is inhibited in vitro by olive oil constituents. Atherosclerosis. 117(1):25–32.

Visioli F, Galli C, Plasmati E, Viappiani S, Hernandez A, Colombo C, Sala A. 2000. Olive phenol hydroxytyrosol prevents passive smoking-induced oxidative stress. Circulation. 102(18):2169–2171.